Multidisciplinary Output Research For Actual and International Issue (MORFAI Journal) ISSN (e): 2808-6635
Volumes 6 No. 6 (2026)

ANALYSIS OF V-CUT TWISTED TAPE ANGLE ON HEAT TRANSFER AND PRESSURE DROP CHARACTERISTICS IN CIRCULAR TUBES

Moniq Pricilianingrum Putri Turnip[1], Damora Rhakasywi[2*], Nicky Yongkimandalan[3]
Mechanical Engineering Department, Faculty of Engineering, Universitas Pembangunan Nasional Veteran Jakarta, Jl. Limo Raya No.80, Limo, Kota Depok, Jawa Barat, 16514, Indonesia
E-mail: 2210311024@mahasiswa.upnvj.ac.id [1], rhakasywi@upnvj.ac.id [2*], nickyyongkimandalan@upnvj.ac.id [3]

Received:05/10/2026 | **Revised** : 12/10/2026 | **Accepted:** 30/10/2026 | **Published:** 26/11/2026

Abstract

This study investigates the effects of single V-cut twisted tape angles on the thermohydraulic performance of a circular tube using Computational Fluid Dynamics (CFD). Numerical simulations used the SST k–ω turbulence model at five Reynolds numbers ranging from 3945 to 9881, with water as the working fluid. We evaluated and compared five V-cut angles (30°, 45°, 60°, 75°, and 90°) with plain-tube and plain twisted tape (PTT) configurations. The reliability of the numerical predictions was assessed through comparisons with experimental measurements and empirical correlations, yielding deviations of less than 10%. The results showed that all V-cut configurations enhanced heat transfer compared with the plain tube and PTT configurations. The 30° V-cut configuration achieved the highest average Nusselt number of 71.589, while the 75° configuration exhibited the highest average friction factor of 0.12509. Based on the Comprehensive Thermal Performance (CTP), the 30° configuration achieved the highest average value of 1.2478, demonstrating the optimal trade-off between improved heat transfer performance and the associated hydraulic losses. Overall, the 30° single V-cut twisted-tape configuration provided the best thermohydraulic performance among the investigated configurations.

Keywords: Heat Exchanger; Computational Fluid Dynamics; Twisted Tape; V-Cut

INTRODUCTION

Heat transfer is fundamental to numerous industrial applications. The efficiency of engineering systems is largely determined by heat exchangers' ability to transfer thermal energy effectively. Heat transfer enhancement has been widely investigated for its contribution to energy conservation, lower operational costs, and improved efficiency of engineering systems (Cabello et al., 2022). Various techniques have been developed to enhance heat transfer performance. One of the most widely applied approaches is passive heat transfer enhancement, which does not require additional external power and is relatively simple to implement in engineering applications (Thapa et al., 2021). Among these techniques, geometric modification through the insertion of twisted tape turbulators into tubes is considered an effective and economical passive method (Varun et al., 2016). Swirling motion and secondary flow structures are generated by these inserts. Improved fluid interaction is then achieved through changes in the thermal boundary layer adjacent to the tube wall, and enhanced convective heat transfer can be achieved through these mechanisms. The resulting flow alterations may also lead to greater hydraulic resistance and an associated rise in pressure drop. Accordingly, the performance of twisted tape inserts should be assessed by accounting for both their heat transfer enhancement capabilities and the accompanying increase in pressure drop (Thote & Singh, 2024).

Numerous studies have investigated geometric modifications of twisted tapes, including perforated twisted tapes and edge-cut twisted tapes. To further modify the flow structure, various cutting geometries have been applied to twisted-tape inserts. V-cut twisted tape (VTT) inserts offer a potential approach to improving the thermohydraulic performance of heat exchangers. The incorporation of V-shaped cuts can generate swirling flow and additional vortical structures, thereby enhancing fluid mixing between the core flow region and the near-wall region (Nakhchi & Esfahani, 2019). Further numerical investigations have explored different V-cut configurations and operating conditions to improve heat transfer performance while managing the associated flow resistance.

LITERATURE REVIEW

Several studies have investigated the thermohydraulic performance of VTT in circular tubes. (Abed et al., 2018) Computational Fluid Dynamics (CFD) simulations were performed to evaluate plain twisted tapes (PTT) and V-cut twisted tapes (VTT) at twist ratios of 4 and 6. Their results demonstrated that VTT tapes produced higher

Nusselt numbers than plain twisted tapes, with a maximum thermal performance factor of approximately 4.45 at a twist ratio of 4. Subsequently, (Chu et al., 2020) experimentally investigated several cut configurations, including U-cut, isosceles V-cut, obtuse V-cut, and successive twisted tapes. Experimental observations have demonstrated that heat transfer characteristics and hydraulic resistance are strongly influenced by the geometric configuration of twisted tape inserts. The obtuse V-cut design attained a CTP of approximately 1.17–1.23 across the investigated Reynolds number range of 4000–10000. The influence of V-cut angle variations was experimentally investigated by (Upadhyay & Kumar Singh, 2022), who examined angles of 15°, 30°, and 45° in a double pipe heat exchanger and identified 45° as the configuration with the best thermohydraulic performance within their investigated range. Meanwhile, (Singh & Kumar, 2022) investigated axial and radial V-cut configurations at the same angles and reported that variations in the cut angle affected the Nusselt number (Nu), friction factor (f), and thermal performance. In addition to angular variations, (Rizqiadinata et al., 2026) investigated the influence of V-cut depth ratio using CFD simulations with the Shear Stress Transport (SST) k-ω turbulence model. It was demonstrated through the investigation that increasing the cut depth enhanced vortex formation, flow recirculation, and fluid mixing, but also increased flow resistance. These findings indicate that twisted tape geometric modifications affect both heat transfer enhancement and pressure drop. Therefore, thermohydraulic performance should be evaluated by considering both parameters simultaneously.

Previous studies have investigated various twisted tape modifications, including variations in twist ratio, cut configurations, depth ratio, and V-cut angle. However, further investigation is still needed into a wider range of V-cut angles in single V-cut twisted tape configurations within circular tubes, particularly to understand the effects of angles greater than 45° on flow characteristics, heat transfer, and pressure losses. Accordingly, this study aims to investigate the effects of single VTT angles: 30°, 45°, 60°, 75°, and 90° on the thermohydraulic characteristics of a circular tube. The Nusselt number is used to determine the extent of heat transfer enhancement, while pressure drop and friction factor are employed to evaluate flow resistance. Furthermore, the Comprehensive Thermal Performance (CTP) is used to assess the trade-off between heat transfer enhancement and the associated hydraulic penalty for each geometric configuration.

METHOD

Geometry Modeling

The computational domain consists of a circular tube equipped with a VTT insert. A three-dimensional model was developed to define the fluid passage and solid boundaries associated with the heat transfer process. The computational model comprises a plain circular tube and a VTT insert. The circular tube has an inner diameter of 21.8 mm and a length of 1000 mm. Meanwhile, the twisted tape insert has a length of 1000 mm, a width of 20 mm, and a thickness of 1 mm, with a twist ratio of 6, and then, for the width of the cut ($2d \tan\frac{\theta}{2}$), adjust the angle size. Fluid flow behavior and thermal performance were evaluated for different V-cut angles while maintaining identical geometric parameters. Five V-cut angles (30°, 45°, 60°, 75°, and 90°) were investigated. The V-cut angle was considered the independent variable, while the tube dimensions and all other twisted tape geometric parameters were kept constant across all configurations. The numerical model of a horizontal circular tube equipped with modified twisted tape inserts is illustrated in Figure 1. Its geometric dimensions are provided in Table 1.

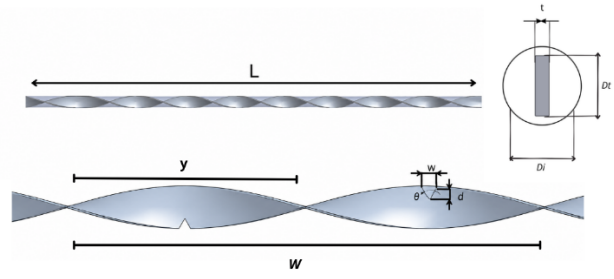


Figure 1. Geometry of the V-cut twisted tape insert

Table 1. Specification of the twisted tape tube

Parameter	Symbol	Dimension (mm)
Tube Length	L	1000
Tube inner diameter	D_i	21.8

OPEN ACCESS

Twisted Tape Length	L	1000
Width of TT	D_t	20
Thickness of TT	t	1.0
Twist ratio	y	6
Helical pitch	W	240
Depth of V-cut	d	5

Governing Equation

The numerical simulation was governed by the conservation equations of mass, momentum, and energy, together with the turbulence transport equations. The continuity equation represents mass conservation for incompressible flow, as expressed in Equation (1). The momentum equation describes fluid motion under the influence of pressure, viscous forces, and body forces, as presented in Equation (2). The energy equation governs heat transfer through convection and thermal diffusion within the fluid, as formulated in Equation (3). Furthermore, turbulence was modeled using the k–ω Shear Stress Transport (SST) model, which involves two additional transport equations: the turbulent kinetic energy equation (k), presented in Equation (4), and the specific dissipation rate equation (ω), presented in Equation (5).

$$\frac{\partial u}{\partial x}+\frac{\partial v}{\partial y}+\frac{\partial w}{\partial z}=0 \quad (1)$$

$$\nabla\cdot\left(\rho\vec{V}\vec{V}\right)=-\nabla P+\mu\nabla^2\vec{V}+\rho\vec{g} \quad (2)$$

$$u\frac{\partial T}{\partial x}+v\frac{\partial T}{\partial y}+w\frac{\partial T}{\partial z}=\alpha\left(\frac{\partial^2 T}{\partial x^2}+\frac{\partial^2 T}{\partial y^2}+\frac{\partial^2 T}{\partial z^2}\right) \quad (3)$$

$$\frac{\partial}{\partial t}(\rho k)+\frac{\partial}{\partial x_i}(\rho k u_i)=\frac{\partial}{\partial x_i}\left[\left(\mu+\frac{\mu_t}{\sigma_k}\right)\frac{\partial k}{\partial x_j}\right]+G_k-Y_k+S_k \quad (4)$$

$$\frac{\partial}{\partial t}(\rho \omega)+\frac{\partial}{\partial x_i}(\rho \omega u_i)=\frac{\partial}{\partial x_i}\left[\left(\mu+\frac{\mu_t}{\sigma_\omega}\right)\frac{\partial \omega}{\partial x_j}\right]+G_\omega-Y_\omega+S_\omega \quad (5)$$

Turbulent flow was modeled using the k-ω SST (Shear Stress Transport) model. The turbulence model is formulated through two additional transport equations: turbulent kinetic energy (k) and specific dissipation rate ω. These equations are used to determine the turbulence characteristics and their effects on the flow field. The near-wall region is treated using the k-ω formulation, whereas k-ε type behavior is adopted in the free-stream region. This hybrid approach enables more accurate predictions of turbulent flow under adverse pressure gradients. (Diwaker & Kumar, 2023)

Mesh Process

An unstructured tetrahedral grid was employed to discretize the computational domain, providing sufficient flexibility to represent the complex geometry of the circular tube integrated with a single VTT insert. Tetrahedral meshing was selected because of its flexibility in discretizing complex three-dimensional geometries (Sarker, 2026). Inflation layers were generated adjacent to the solid walls to provide finer mesh resolution in the near-wall regions, where significant velocity and temperature gradients occur. Inflation layers were applied to the fluid domain using the first layer thickness option. The validity of numerical predictions is strongly influenced by the quality of the mesh employed in CFD simulations. Therefore, a grid independence test was conducted to evaluate the stability of the simulation results with respect to variations in mesh density. Furthermore, the Grid Convergence Index (GCI) method proposed by (Roache, 1994) was employed to quantify the numerical uncertainty associated with grid refinement. Mesh independence was assessed for the plain-tube model, with the corresponding verification results summarized in Table 2.

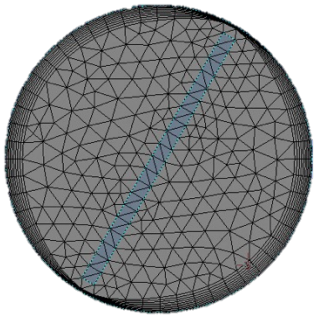


Figure 2. Meshing of pipe with twisted tape insert

$$r = \frac{h_2}{h_1} \quad (6)$$

$$\overline{p} = \frac{ln\left(\frac{f_3 - f_2}{f_2 - f_1}\right)}{(r^{\overline{p}} - 1)} \quad (7)$$

$$GCI_{fine} = \frac{F_s \ |\epsilon|}{(r^{\overline{p}} - 1)} \quad (8)$$

$$GCI_{coarse} = \frac{F_s \ |\epsilon| \ r^{\overline{p}}}{(r^{\overline{p}} - 1)} \quad (9)$$

$$\frac{GCI_{fine}}{GCI_{coarse}r^{\overline{p}}} \approx 1 \quad (10)$$

$$f\ r_{h=0} = f_1 + \frac{(f_1 - f_2)}{(r^{\overline{p}} - 1)} \quad (11)$$

$$\epsilon = \frac{f_{n+1} - f_n}{f_n} \quad (12)$$

Table 2. Mesh Independent Test

Mesh Category	Fine	Medium	Coarse
Elements	1.351.106	1.002.086	716.833
Nu	32.81	32.88	33.40
r		1.30	
p		7.64	
GCI_{fine}		0.041%	
GCI_{coarse}		0.308%	
GCI ratio		1.00	
Error	0.03%	0.25%	1.83%

Boundary Condition

The prescribed boundary conditions were established to simulate fluid motion and thermal behavior inside the circular tube. A velocity inlet boundary condition was applied, with inlet velocities varying from 0.181 to 0.455 m/s, representing to Reynolds numbers of 3945, 5425, 6904, 8402, and 9881. The working fluid was liquid water at an inlet temperature of 25°C. A uniform heat flux of 1200 W/m² was applied to the heated tube wall, while the twisted-tape surfaces and the remaining unheated tube walls were assumed to be adiabatic. Stainless steel 304 was selected as the material for the twisted tape insert. The thermophysical properties of water are listed in Table 4, whereas the corresponding data for stainless steel 304 are provided in Table 3.

Table 3. Material Properties of Stainless Steel 304

Properties	Value
Density, p	8030 kg/m^3
Thermal conductivity, k	16.27 W/m.K
Specific heat, Cp	502.48 J/kg.K

OPEN ACCESS

Table 4. Material Properties of Water

Properties	Value
Density, p	998.2 Kg/m^3
Thermal conductivity, k	0.6 W/m.K
Specific heat, Cp	4182 J/Kg.K
Dynamic viscosity, μ	0.001003 Kg/m.s

Data Collection

The Reynolds number was used in this study to characterize the flow regime under different fluid velocity conditions. It was calculated using the following equation:

$$\text{Re} = \frac{\rho.v.D_i}{\mu} \quad (13)$$

Fluid density (ρ) was adopted as one of the parameters in determining the Reynolds number, measured in Kg/m³, the mean velocity (v) expressed in m/s, represents the tube's internal diameter (D_i) measured in meters, while (μ) the dynamic viscosity of the working fluid measured in Kg/m.s.

The convective heat transfer coefficient is expressed mathematically as follows:

$$h = \frac{Q}{\Delta T\,.\,A} \quad (14)$$

The parameter (h) denotes the convective heat transfer coefficient, expressed in W/m^2.K, was determined based on the heat transfer rate (Q), also measured in W/m^2, heat transfer area (A), and the logarithmic mean temperature difference (ΔT) expressed in K.

ΔT is the logarithmic mean temperature difference. The ΔT is defined by:

$$\Delta T = \frac{T_{out} - T_{in}}{ln\left[\frac{T_w - T_{in}}{T_w - T_{out}}\right]} \quad (15)$$

The parameter (T_w) represents the average surface temperature measured at the interface between the tube wall and the flowing fluid (K), whereas T_b denotes the bulk mean fluid temperature (K), which is determined using the following equation:

$$T_b = \frac{T_{in} + T_{out}}{2} \quad (16)$$

The dimensionless Nusselt number (Nu) and Darcy friction factor (f) are determined using the tube's internal diameter as the characteristic length, according to the following equations:

$$\text{Nu} = \frac{hD}{k} \quad (17)$$

$$\text{f} = \frac{\Delta P}{\frac{\rho.u^2}{2}} \cdot \frac{D}{L} \quad (18)$$

Meanwhile, the Darcy friction factor was determined from the pressure drop (ΔP), which denotes the pressure reduction measured in Pa, mean flow velocity (u), and (D_i) measured in m, tube inner diameter heated tube length in and (L) represents the m.

The heat exchanger's performance is evaluated using the Comprehensive Thermal Performance (CTP), a dimensionless parameter that quantifies the trade-off between enhanced heat transfer and the associated pressure drop. The mathematical formulation of CTP is presented in the following equation:

$$\text{CTP} = \frac{Nu/Nup}{(\frac{f}{fp})^{1/3}} \quad (19)$$

RESULTS AND DISCUSSION

Validation

Numerical model validation was performed using a plain tube configuration without a twisted tape insert. Model validation was performed through comparisons of CFD-derived results with experimental data published by (Chu et al., 2020) and predictions obtained from established empirical correlations. The Nusselt number (Nu) was evaluated using the Gnielinski correlation, as presented in Equation (20) (Chu et al., 2020) while the friction factor was assessed using the Filonenko correlation, as presented in Equation (21) (Taler, 2016).

$$Nu = \frac{\left(\frac{f}{8}\right)(Re-1000)Pr}{1+12.7\sqrt{f/8}\,(Pr^{2/3}-1)} \quad (20)$$

$$f = (1.82logRe - 1.64)^{-2} \quad (21)$$

Where P_r is the Prandtl number, expressed as:

$$P_r = \frac{\mu C_p}{k} \quad (22)$$

Where k is the thermal conductivity of the fluid, measured in W/m² K. The specific heat capacity of the fluid is denoted by Cp, expressed in J/kg.K, whereas μ represents its dynamic viscosity, measured in kg/m.s.

Figure 3 presents the comparison between the numerical predictions and the experimental results obtained from the investigation of (Chu et al. 2020), which served as the basis for the first validation stage. The second validation test was conducted using established empirical correlations. For the Nusselt number, the average percentage deviation between the simulation results and the experimental data was 4.66%, while the deviation obtained using the Gnielinski correlation was 5.92%. Meanwhile, for the friction factor, the average percentage deviation from the experimental data was 4.89%, whereas the deviation obtained using the Filonenko correlation was 4.95%. All deviation errors were relatively small and remained well below the adopted validation tolerance of 10%. Good agreement was obtained between the plain-tube numerical predictions, experimental measurements, and established empirical correlations. The validated model was subsequently considered suitable for further numerical analysis.

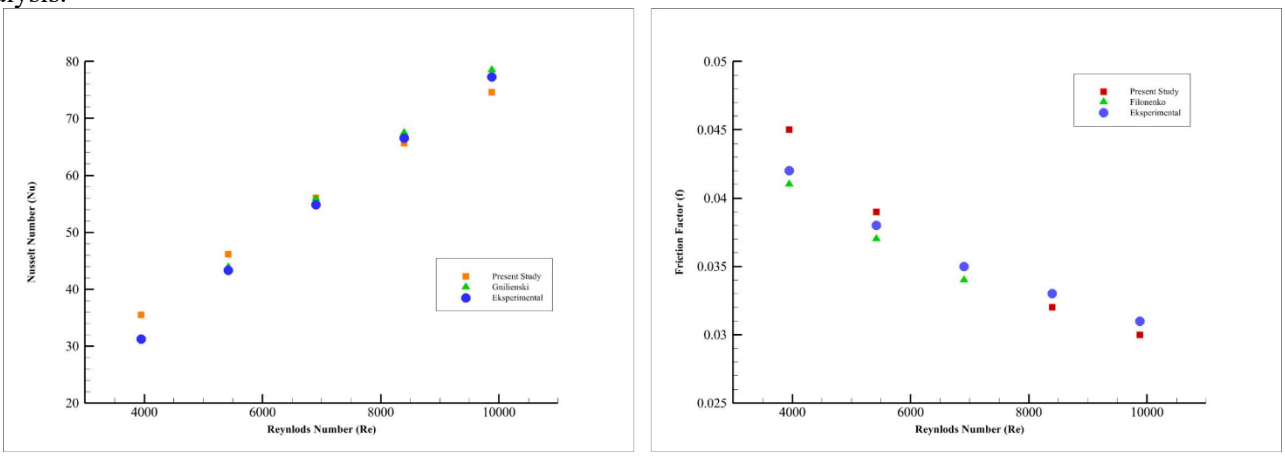


Figure 3. (a) Nusselt Number Validation and (b) Friction Factor Validation

Analysis

As illustrated in Figure 4, the Nusselt number (Nu) increased with Reynolds number (Re) across all configurations, indicating an enhancement in convective heat transfer within the circular tube. For the plain tube configuration, the Nu value increased from 35.47 at Re = 3945 to 74.60 at Re = 9881. Meanwhile, the PTT insert produced higher Nu values, increasing from 46.04 to 86.28 over the same Reynolds number range. The twisted tape geometry generates rotational motion within the fluid. Enhanced mixing is produced by this mechanism, accompanied by disturbances in the thermal boundary layer adjacent to the tube wall.

Furthermore, the incorporation of a single VTT insert resulted in greater heat transfer enhancement than both the plain-tube and PTT configurations. Based on the average Nu values across the five Reynolds numbers, the 30° V-cut configuration achieved the highest value of 71.589, followed by the 45° configuration at 71.415, the 60° configuration at 71.141, the 75° configuration at 70.955, and the 90° configuration at 70.898. The highest average Nusselt number was recorded for the 30° V-cut configuration, establishing this geometry as the most effective design for thermal enhancement among the tested angles. The development of secondary vortical structures may be facilitated by V-cut modifications. Enhanced fluid interaction is consequently expected between the central flow and the regions adjacent to the tube wall.

The simulation results show that the friction factor (f) decreased with increasing Reynolds number across all configurations. For the plain tube, the friction factor decreased from 0.045 to 0.03075, whereas the PTT configuration exhibited higher values, decreasing from 0.14695 to 0.09116 over the same Reynolds number range. This increase in flow resistance is attributed to the twisted tape insert, which induces swirling flow and enhances interactions between the fluid, the insert, and the tube wall. Furthermore, the single VTT configurations generally exhibited higher friction factors than the PTT configuration. Based on the average values across the five Reynolds numbers, the 75° V-cut configuration produced the highest friction factor (0.12509), followed by 30° (0.11755), 45° (0.11742), 60° (0.11739), and 90° (0.11705). The relatively high average value for the 75° configuration was

OPEN ACCESS

primarily influenced by its friction factor of 0.19084 at Re = 3945. In contrast, the 90° configuration yielded the lowest average friction factor, indicating the lowest flow resistance among the investigated V-cut angles.

The analysis of the Nu and f indicates that each twisted tape configuration exhibits different heat transfer and flow resistance characteristics at different Reynolds numbers. An enhancement in heat transfer efficiency does not always correspond to a decrease in hydraulic resistance. The thermohydraulic performance of each configuration is evaluated through the CTP parameter by accounting for thermal enhancement and the associated pressure losses. The most favorable design can subsequently be identified from this assessment.

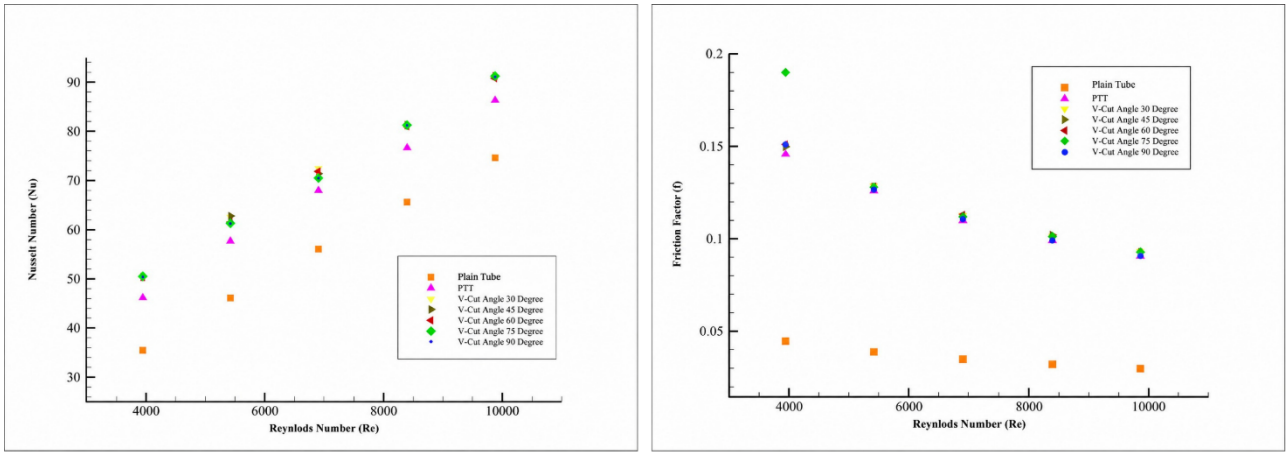


Figure 4. Variation of Nusselt number (a) and Friction factor (b) with Reynolds number for Plain Tube, PTT, and V-cut twisted tape (VTT) configurations with different V-cut angles

Based on the simulation results, Figure 5 illustrates variations in CTP across the investigated Reynolds numbers (Re) and twisted tape configurations. CTP values above 1 were recorded for every V-cut configuration throughout the investigated Reynolds number range, demonstrating that the thermal improvement was greater than the corresponding increase in hydraulic resistance. For the PTT configuration, the CTP value increased from 0.6092 at Re = 3945 to 1.1375 at Re = 9881. CTP values below 1 at Re = 3945, 5425, and 6904 indicate that the heat transfer enhancement was insufficient to compensate for the increased flow resistance. However, at Re = 8402 and 9881, the CTP values exceeded 1, indicating improved thermohydraulic performance at higher Reynolds numbers. Meanwhile, the single VTT configurations exhibited consistently higher CTP values than the PTT configuration under all investigated conditions. For each Reynolds number, the highest CTP value varied with the V-cut angle. The 30° configuration achieved the highest value of 1.3481 at Re = 3945, while the 45° configuration recorded the highest value of 1.2832 at Re = 5425. At Re = 6904, the 30° configuration again produced the highest CTP value of 1.2412. In contrast, the highest values at Re = 8402 and 9881 were obtained with the 90° and 75° configurations, reaching 1.1969 and 1.1807, respectively.

These differences indicate that the V-cut angle associated with the highest thermohydraulic performance varies depending on the Reynolds number. Based on the average CTP values across the five Reynolds numbers, the 30° V-cut configuration achieved the highest value of 1.2478, followed by the 45° (1.2464), 60° (1.2418), 90° (1.2410), and 75° (1.1849) configurations. Accordingly, the 30° V-cut configuration exhibited the best overall performance based on the average CTP value, providing a favorable balance between heat transfer enhancement, as indicated by the Nusselt number, and flow resistance, represented by the friction factor. The results also indicate that the relatively high flow resistance of the 75° configuration at lower Reynolds numbers contributed to a considerable reduction in its CTP value. Overall, the single VTT insert with a 30° angle demonstrated the most favorable thermohydraulic performance among all the investigated configurations.

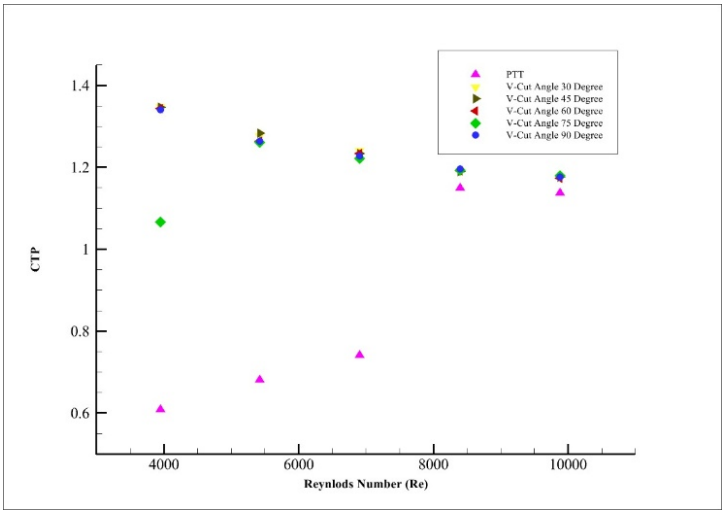


Figure 5. Results of the CTP with varied Reynolds number for PTT and V-cut Twisted Tape configurations with different V-cut angles

Figure 6 At Re = 3945, distinct velocity distributions were observed across the examined geometries. A relatively uniform flow pattern was obtained in the plain tube, with peak velocities concentrated along the central axis and a gradual reduction toward the inner wall. This decrease in velocity is related to the effect of viscous forces, as illustrated by the contour distribution. This indicates a relatively symmetrical velocity profile without disturbances from additional inserts. With the addition of a PTT insert, the velocity distribution changes due to the formation of swirling flow induced by its twisted geometry. The insert alters the flow trajectories and generates centrifugal effects that drive the fluid toward the near-wall region. Consequently, the velocity distribution becomes more complex, as indicated by variations in the contour patterns above and below the insert, along with the formation of low-velocity regions around its surfaces. These observations indicate that the addition of a turbulator intensifies flow disturbances and promotes fluid mixing compared with the plain tube configuration.

Furthermore, the single VTT configurations exhibit changes in velocity distribution around the V-cut regions compared with the PTT configuration. The presence of these cuts provides additional pathways for fluid to pass between both sides of the twisted-tape insert, allowing flow interactions between the upper and lower regions of the insert. Secondary vortical structures may be generated by alterations in the fluid trajectory. Improved mixing is also expected between the central stream and the wall-adjacent layer. For the V-cut angles of 30°, 45°, 60°, 75°, and 90°, the overall velocity distributions exhibit relatively similar characteristics, although local variations occur around the cut regions and insert edges due to differences in V-cut geometry. These variations indicate that the V-cut angle influences flow interactions and velocity distribution within the tube. This observation is consistent with the quantitative Nusselt number results, which show higher values for all V-cut configurations than for the plain tube and PTT configurations. Therefore, V-cut modifications not only alter the velocity distribution but may also enhance fluid mixing, thereby promoting convective heat transfer within the circular tube.

OPEN ACCESS

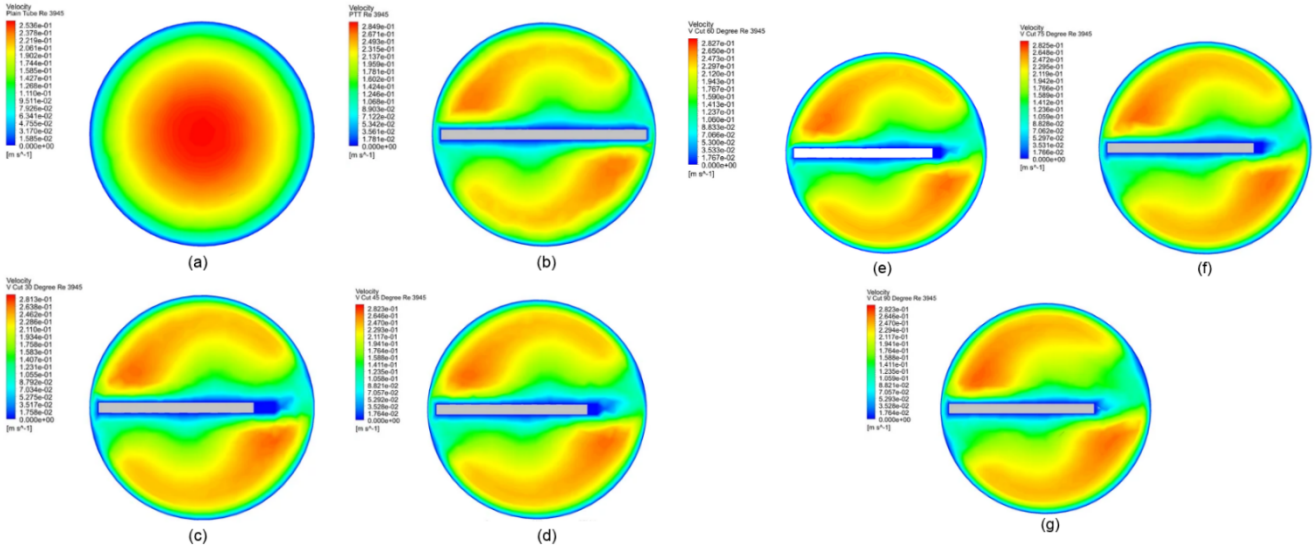


Figure 6. Velocity contour distribution at the tube cross section for (a) Plain Tube, (b) PTT, and V-cut twisted tape (VTT) configurations with V-cut angles of (c) 30°, (d) 45°, (e) 60°, (f) 75°, and (g) 90° at Re = 3945 and a distance of 480 mm from the inlet.

The temperature contour can be seen in Figure 7. At a Reynolds number (Re) of 3945, differences can be observed in the temperature distribution patterns among the investigated configurations. In the plain-tube configuration, as shown in Figure (a), the temperature distribution exhibits a relatively radially symmetrical pattern, with higher temperatures concentrated near the tube wall, indicated by yellow to red contours, while lower temperatures are observed in the core region, indicated by blue contours. A thermal gradient is observed between the fluid adjacent to the heated wall and the central portion of the tube. Following the insertion of PTT, as shown in Figure (b), the temperature distribution becomes less uniform due to the presence of the insert, which alters the flow trajectories and induces swirling flow. A non-uniform radial temperature profile is observed around the twisted tape insert. Its distribution is governed by the altered fluid trajectories along the insert surfaces. The observed variations demonstrate that the turbulator alters the flow-mixing characteristics and modifies the thermal energy distribution throughout the tube.

Furthermore, the temperature distribution in the single VTT configurations, as shown in Figures (c)–(g), exhibits patterns relatively similar to those of the PTT configuration, although changes in the contour patterns can be observed around the V-cut regions. The presence of these cuts allows potential flow exchange between the upper and lower sides of the twisted tape insert, which may enhance mixing between fluid regions at different temperatures. This is reflected in the asymmetric temperature contours and variations in color gradients across several regions of the tube cross section. For the V-cut angles of 30°, 45°, 60°, 75°, and 90°, the differences in temperature distribution are relatively small, although local variations in the distribution of high and low temperature regions occur due to differences in cut geometry. Overall, the addition of V-cuts produces a more complex temperature distribution than that observed in the plain tube configuration. This behavior is consistent with the previously discussed Nusselt number results, which indicate that all V-cut configurations achieve higher values than the plain tube and PTT configurations. Therefore, V-cut modifications may enhance fluid mixing and promote convective heat transfer within the circular tube.

OPEN ACCESS

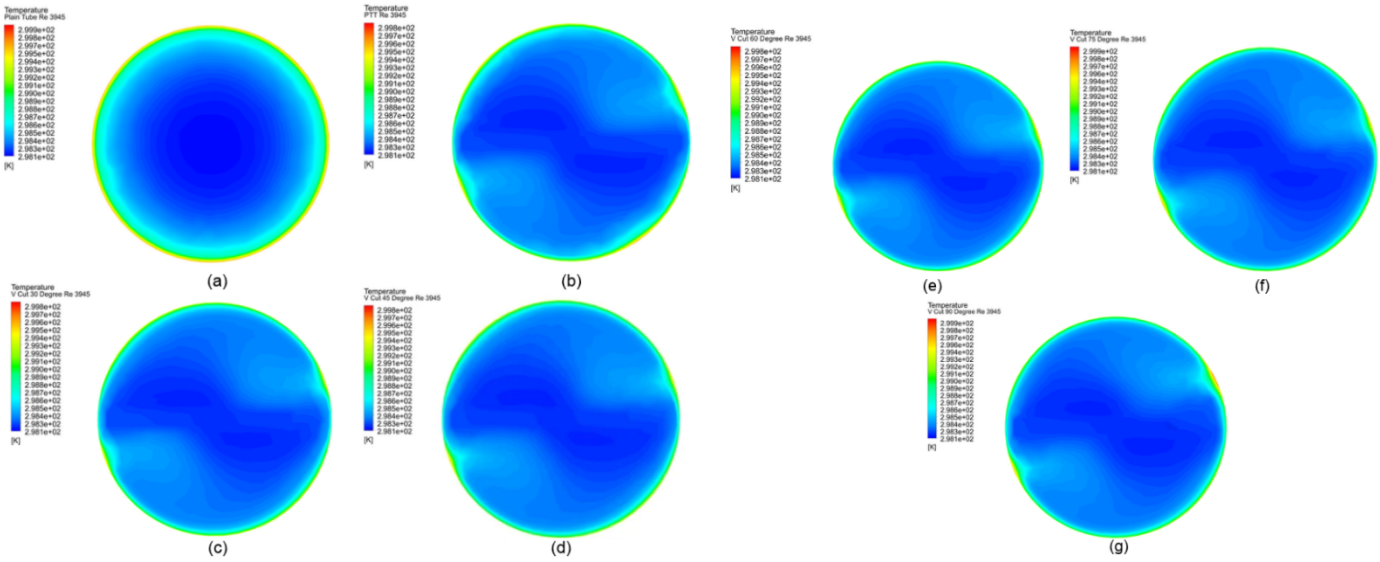


Figure 7. Temperature contour distribution at the tube cross section for (a) Plain Tube, (b) PTT, and V-cut twisted tape (VTT) configurations with V-cut angles of (c) 30°, (d) 45°, (e) 60°, (f) 75°, and (g) 90° at Re = 3945 and distance 480 mm from the inlet.

Streamline visualization was used to examine fluid flow trajectories within the tube, shown in Figure 8. In the plain tube configuration, the streamlines follow relatively straight and parallel paths from the inlet to the outlet, indicating limited flow disturbances and fluid mixing between the core and near-wall regions. In contrast, the PTT insert induces swirling flow and generates a tangential velocity component, resulting in more complex flow trajectories and enhanced fluid mixing. The single VTT configurations further modify the flow patterns around the cut regions by providing additional pathways for fluid exchange between both sides of the insert. These changes may promote momentum exchange and secondary vortex formation, leading to enhanced fluid interaction between the core flow and the regions adjacent to the tube wall. More pronounced flow deflections are observed in the 75° configuration than in the 30° configuration, indicating stronger interactions between the fluid and insert surfaces.

Overall, the PTT and V-cut modifications produce more complex flow structures than the plain tube. At Re = 3945, the 30° configuration achieves a Nu of 50.273 and a CTP of 1.3481, whereas the 75° configuration yields a slightly higher Nu of 50.496 but a lower CTP of 1.0672. This difference is associated with the greater flow resistance of the 75° configuration, as reflected by its friction factor of 0.19084 compared with 0.15041 for the 30° configuration. These findings suggest that the 75° configuration offers a marginally higher level of heat transfer enhancement, while the 30° configuration achieves better thermohydraulic performance due to its lower hydraulic penalty.

OPEN ACCESS

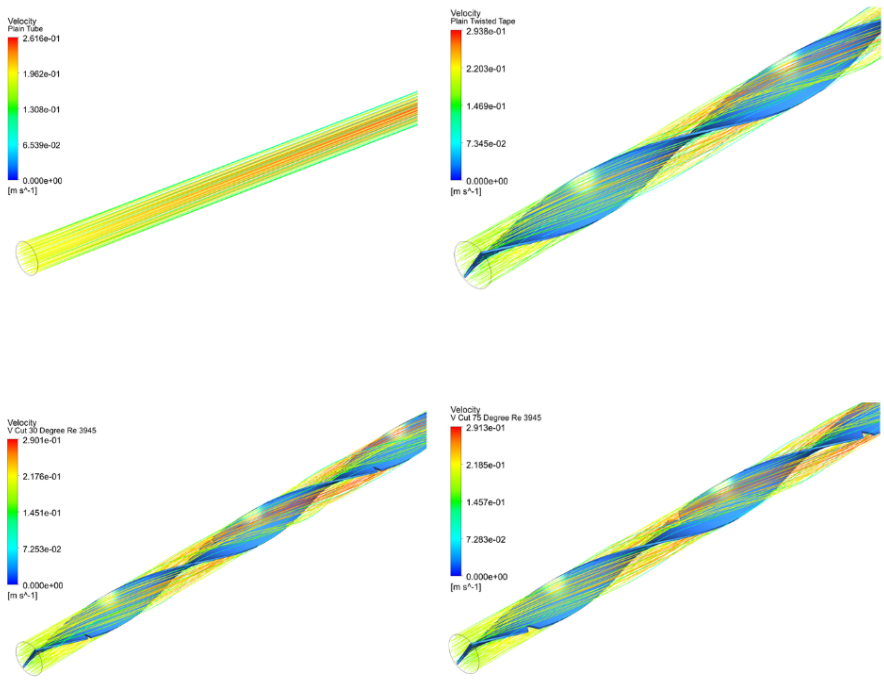


Figure 8. Velocity streamlines at the tube cross section for (a) Plain Tube, (b) PTT, and V-cut twisted tape (VTT) configurations with V-cut angles of (c) 30°, (d) 45°, (e) 60°, (f) 75°, and (g) 90° at Re = 3945.

CONCLUSION

This study investigated the effects of single VTT angle variations on the thermohydraulic characteristics of a circular tube using Computational Fluid Dynamics (CFD). The numerical model validation showed deviations of less than 10% from the experimental data and empirical correlations, indicating good agreement and demonstrating the model's suitability for evaluating the thermohydraulic characteristics of different twisted-tape configurations. The numerical findings revealed a consistent increase in the Nusselt number as the Reynolds number increased for all configurations investigated. The incorporation of a PTT insert resulted in greater heat transfer performance relative to the plain-tube configuration, while the V-cut modifications provided further enhancement over both configurations. An average Nusselt number of 71.589 was obtained for the 30° V-cut geometry across the five Reynolds number conditions, representing the highest value among the configurations examined. Meanwhile, the friction factor exhibited an overall declining trend as the Reynolds number increased, with the 75° V-cut configuration exhibiting the highest average flow resistance due to its relatively high friction factor at lower Reynolds numbers. The Comprehensive Thermal Performance (CTP) evaluation revealed that the 30° V-cut configuration achieved the highest average value of 1.2478, followed by the 45° (1.2464), 60° (1.2418), 90° (1.2410), and 75° (1.1849) configurations. Furthermore, the velocity contours, temperature contours, and streamline visualizations at Re = 3945 revealed changes in velocity and temperature distributions, as well as flow trajectories, resulting from the addition of twisted-tape inserts and V-cut modifications. Overall, the single VTT configuration with a 30° angle demonstrated the best thermohydraulic performance based on the highest average CTP value, making it the most favorable configuration among those investigated.

REFERENCES

Abed, A. M., Sh Majdi, H., Hussein, Z., Fadhil, D., & Abdulkadhim, A. (2018). Numerical analysis of flow and heat transfer enhancement in a horizontal pipe with P-TT and V-Cut twisted tape. Case Studies in Thermal Engineering, 12, 749–758. https://doi.org/10.1016/j.csite.2018.10.004

Cabello, R., Plesu Popescu, A. E., Bonet-Ruiz, J., Curcó Cantarell, D., & Llorens, J. (2022). Heat transfer in pipes with twisted tapes: CFD simulations and validation. Computers and Chemical Engineering, 166(August). https://doi.org/10.1016/j.compchemeng.2022.107971

OPEN ACCESS

Chu, W. X., Tsai, C. A., Lee, B. H., Cheng, K. Y., & Wang, C. C. (2020). Experimental investigation on heat transfer enhancement with twisted tape having various V-cut configurations. Applied Thermal Engineering, 172(December 2019), 115148. https://doi.org/10.1016/j.applthermaleng.2020.115148

Diwaker, M. K., & Kumar, A. (2023). Thermo-Hydraulic Performance of Tube Type Heat Exchanger with Semi-Circular Cut Twisted Tape Insert: A Numerical Exploration. Journal of Heat and Mass Transfer Research, 10(1), 159–170. https://doi.org/10.22075/jhmtr.2023.30445.1438

Nakhchi, M. E., & Esfahani, J. A. (2019). Performance intensification of turbulent flow through heat exchanger tube using double V-cut twisted tape inserts. Chemical Engineering and Processing - Process Intensification, 141(May), 107533. https://doi.org/10.1016/j.cep.2019.107533

Rizqiadinata, F., Rhakasywi, D., & Yongkimandalan, N. (2026). NUMERICAL INVESTIGATION OF DEPTH RATIO EFFECTS ON THERMOHYDRAULIC PERFORMANCE OF A HEAT EXCHANGER WITH V-CUT TWISTED TAPE. 6(5), 7591–7602.

Roache, P. J. (1994). Perspective: A method for uniform reporting of grid refinement studies. Journal of Fluids Engineering, Transactions of the ASME, 116(3), 405–413. https://doi.org/10.1115/1.2910291

Sarker, D. (2026). Comparative CFD assessment of mesh topology and turbulence models for twisted-tape-induced convection. Advances in Mechanical Engineering, 18(10), 1–16. https://doi.org/10.1177/16878132261496098

Singh, S. K., & Kumar, A. (2022). Experimental study of heat transfer and friction factor in a double pipe heat exchanger using twisted tape with dimple inserts. Energy Sources, Part A: Recovery, Utilization and Environmental Effects, 47(1), 7951–7980. https://doi.org/10.1080/15567036.2021.1927248

Taler, D. (2016). A new heat transfer correlation for transition and turbulent fluid flow in tubes. International Journal of Thermal Sciences, 108, 108–122. https://doi.org/10.1016/j.ijthermalsci.2016.04.022

Thapa, S., Samir, S., Kumar, K., & Singh, S. (2021). A review study on the active methods of heat transfer enhancement in heat exchangers using electroactive and magnetic materials. Materials Today: Proceedings, 45(xxxx), 4942–4947. https://doi.org/10.1016/j.matpr.2021.01.382

Thote, S. A., & Singh, N. P. (2024). Improvement of Heat Transfer Through Use of Twisted Tape Inserts: A Review. Journal of Engineering, Project, and Production Management, 14(1), 1–9. https://doi.org/10.32738/JEPPM-2024-0007

Upadhyay, C., & Kumar Singh, S. (2022). Experimental Study of Heat transfer and friction factor in Double pipe Heat Exchanger using Twisted Tape with different groove angle of V-cut at constant depth. International Journal of Research in Engineering and Science (IJRES) ISSN, 10(1), 12–18. www.ijres.org

Varun, Garg, M. O., Nautiyal, H., Khurana, S., & Shukla, M. K. (2016). Heat transfer augmentation using twisted tape inserts: A review. Renewable and Sustainable Energy Reviews, 63, 193–225. https://doi.org/10.1016/j.rser.2016.04.051

OPEN ACCESS